INVESTIGATIONS OF FOUR-PORT CIRCULATOR UTILIZING CYLINDRICAL FERRITE COUPLED LINE JUNCTION

Adam Kusiek[*], Wojciech Marynowski, and Jerzy Mazur

Faculty of Electronics, Telecommunications and Informatics, Gdansk University of Technology, Gdansk, Poland

Abstract—In this paper the numerical and experimental investigations of four-port circulator utilizing longitudinally magnetized cylindrical ferrite coupled lines (CFCL) section are presented for the first time. In comparison to earlier models the proposed structure of circulator utilizes multilayer magic-T junction cascaded with cylindrical ferrite section of $\pi/4$ Faraday angle. The advantage of utilization of cylindrical section over the planar one is the possibility to design shorter ferrite junctions ensuring lower insertion losses. Moreover, the multilayer magic T-junction allows to improve performance of the proposed circulator by omitting the bandwidth limitation which exists in commonly used hybrid couplers with air-bridges. In the analysis of CFCL junction the full wave hybrid approach combining finite difference frequency domain method with method of moments and mode matching technique is applied. The planar feeding structures of circulator are designed with the use of commercial software. The simulated results of the entire circulator are compared with the measurement results of the fabricated prototype and a good agreement is achieved.

1. INTRODUCTION

The novel class of integrated nonreciprocal devices such as isolators or circulators are the one realized with the use of longitudinally magnetized ferrite coupled lines section (FCL) [1–11]. Significant interest in these devices results from their advantages such as weak biasing magnetic field and wide operation bandwidth [2].

   The basic part of the ferrite coupled line (FCL) devices is longitudinally magnetized FCL section composed of two coupled lines

placed on ferrite substrate [11–13]. According to the coupled-mode model [12] in such section the gyromagnetic coupling occurs resulting in Faraday rotation effect. In order to construct devices such as circulators [1–6, 9, 11], gyrators [7] or isolators [8, 10] the FCL section has to be cascaded with reciprocal section providing input signals to the FCL which are either in phase or out of phase.

One group of FCL devices are four-port circulators [2, 9, 11]. In this group two types of circulator can be distinguished. One type comprises of four-port circulators that are obtained by cascading two three-port circulators (see Figs. 1(a)–1(c)). The other type of circulators is composed of FCL junction cascaded with magic-T junction (see Fig. 1(d)). The main advantage of the first type is easy to design planar feeding circuit [14–20]. However, taking into account that such structures involve two ferrite sections, the overall dimensions of four-port device and total insertion losses become high. The second type utilizes only a single ferrite section and as a result the total dimensions of the structure and insertion losses are lower. However, such circulators require feeding structures ensuring even and odd excitation of ferrite junction (e.g., hybrid couplers [11] or magic-T junction [21, 22]), which realization is more complex in planar line technology.
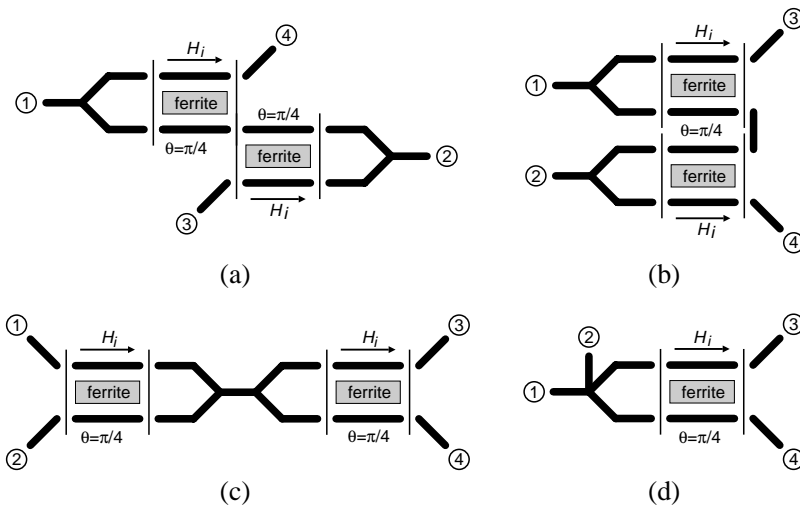

Figure 1. Basic configurations of four-port FCL circulators utilizing (a) two cascaded three-port circulators, (b) two folded three-port circulators, (c) two cascaded three-port circulators with joined coupled lines, and (d) single ferrite section cascaded with magic-T junction.

Up to now, four-port FCL circulators have been realized in microstrip [9, 11] or stripline [2] technology. In the case of circulators from Figs. 1(a)–1(c) the best performance was observed for the structure of circulator from Fig. 1(a) for which the average insertion losses were 3 dB with isolation better than 20 dB [9]. In the case of structure from Fig. 1(d) the circulator utilizing hybrid coupler [11] was designed and fabricated. For the fabricated prototype the insertion losses were not better than 4 dB with isolation about 12 dB. Moreover, the existence of air-bridge in hybrid coupler significantly limits the bandwidth of the proposed circulator.

In this paper we present for the first time the four-port circulator utilizing $\pi/4$ cylindrical ferrite coupled line junction. The proposed circulator is obtained by cascading multilayer magic-T junction with CFCL junction and output transformer from coupled cylindrical slotlines to uncoupled microstrip lines. The advantage of utilization of cylindrical section over planar one is the possibility to design shorter ferrite junctions ensuring lower insertion losses. Moreover, the multilayer T-junction allows to improve performance of the proposed circulator by omitting the bandwidth limitation which exists in commonly used hybrid couplers with air-bridges. To design CFCL junction with $\pi/4$ Faraday rotation angle, the hybrid approach combining finite-difference frequency-domain technique, method of moments and mode matching technique (FDFD/MoM/MM) is applied. Utilizing commercial software HFSS we validate results of FDFD/MoM/MM and design multilayer reciprocal circuits of the structure. The overall scattering parameters of the circulator are obtained by cascading the S-matrices of the feeding circuits and CFCL junction. The simulated results are verified by own measurements of fabricated prototype.

2. S-MATRIX OF CFCL JUNCTION

In the analysis of CFCL junction we utilize the hybrid technique combining finite-difference frequency-domain method, method of moments and mode matching technique (see Fig. 2). At first step of our approach the propagation coefficients and field distributions of fundamental modes occurring in dielectric and ferrite guides are calculated using FDFD/MoM. This is done by determining impedance representation of an artificial cylinder enclosing inner dielectric/ferrite rod with the use of FDFD technique. Then the obtained discrete solution is combined with the analytical fields in the outer region of the artificial cylinder using MoM [23]. As a result a set of homogenous equations is obtained which solution are propagation coefficients and
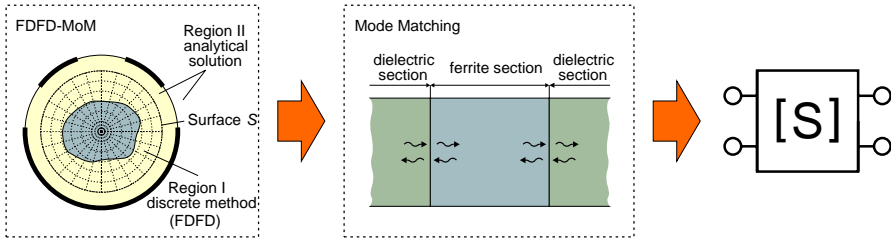
Figure 2. Basic steps of FDFD/MoM/MM approach.

field distributions of modes occurring in the investigated guide. The main advantage of FDFD/MoM technique is its application to the analysis of guides loaded with dielectric/ferrite rod of arbitrary shape (e.g., cylindrical, elliptical). Moreover, in the case of ferrite guides any bias magnetic field (e.g., four-pole bias magnetic field) can be taken into account. The detailed description of FDFD/MoM technique is presented in Section 2.1.

Next, using described in [3] MM technique we determine the scattering matrix of the CFCL junction (see Fig. 2). Such junction is realized as a cascade connection of dielectric, ferrite and another dielectric sections of the same geometry differing only with the material parameters of the inner rod. The transverse electromagnetic fields in the dielectric sections are expanded with the use of even and odd dominant isotropic modes. The transverse electromagnetic fields in the ferrite section are expanded by two forward and backward going dominant ferrite modes. By applying the continuity conditions for the tangential field components at the both interfaces between dielectric and ferrite sections, we formulate the scattering matrix including the response of input even and odd isotropic modes. Next, using the symmetry of isotropic waves, the even-odd **S**-matrix is rearranged in terms of the port waves and finally we obtain the complete scattering matrix of 4-port FCL junction.

2.1. FDFD/MoM Approach

The considered cylindrical guide is presented in Fig. 3. We assume that the guide is loaded with dielectric rod of arbitrary cross-section or ferrite rod of arbitrary cross-section with any-directed biasing magnetic field. In the proposed approach we define artificial cylindrical surface $\mathcal{S}$ surrounding the centrally situated dielectric/ferrite rod in the guide, which divides the structure into inner and outer region. In the outer region the fields are expressed using analytical relations [23].
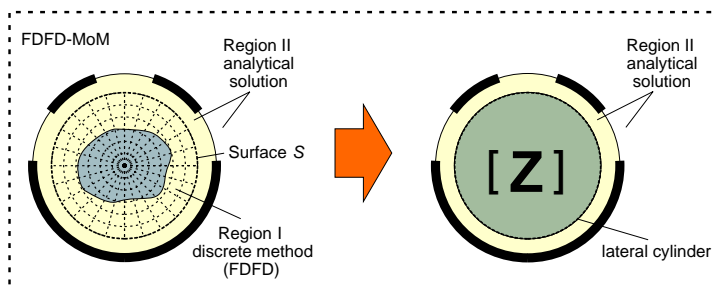
Figure 3. Impedance representation of artificial cylinder enclosing ferrite rod.

In the inner region the analytical solution is difficult to find due to the complexity of structure, hence the more universal discrete FDFD technique is applied.

The tangential components of electric and magnetic fields on the surface $\mathcal{S}$ can be defined as follows:

$$E_{z,\varphi}^{I}(R,\varphi,z) = \sum_{m=-M}^{M} C_m^{E_{z,\varphi}} e^{j(m\varphi - \beta z)}, \tag{1}$$

$$H_{z,\varphi}^{I}(R,\varphi,z) = \sum_{m=-M}^{M} D_m^{H_{z,\varphi}} e^{j(m\varphi - \beta z)}. \tag{2}$$

where β is propagation coefficient. The unknown expansion coefficients $C_m^{E_{z,\varphi}}$ and $D_m^{H_{z,\varphi}}$ can be related utilizing impedance matrix as follows:

$$\mathbf{C} = \mathbf{Z}\mathbf{D}. \tag{3}$$

The impedance matrix defines the relation between electric and magnetic tangential field components on the surface $\mathcal{S}$. This allows us to treat the artificial cylinder as a homogeneous rod with the boundary conditions defined by **Z**-matrix. Combining impedance matrix with the analytical solution in the outer region the propagation coefficients and field distributions of the modes occurring in the considered guide can be easily determined [23].

For the considered problem **Z** matrix is determined with the use of FDFD technique. This approach was previously applied in [24] to the analysis of waveguide structures and scattering problems. Here this technique is modified to the analysis of cylindrical guides and only its brief description will be here presented. Since, the investigated guide is homogeneous along z-axis the analytical variation of fields along z-axis is assumed in the form $e^{-j\beta z}$. As a result the computational domain

is discretized only in z-const plane. The Maxwell equations written in a discrete form are expressed as follows:

$$\mathbf{P}_1\mathbf{D}_1(\mathbf{QE} + \mathbf{Q}_b\mathbf{E}_b) = j\omega\mu_0\boldsymbol{\mu}_r\mathbf{S}_1\mathbf{H}, \tag{4}$$

$$\mathbf{P}_2\mathbf{D}_2\mathbf{H} = j\omega\varepsilon_0\boldsymbol{\varepsilon}_r\mathbf{S}_2\mathbf{E}, \tag{5}$$

where $\mathbf{P}_{1,2}$ are the matrices of derivatives, $\mathbf{Q}, \mathbf{Q}_b$ the matrices of projection, $\mathbf{D}_{1,2}, \mathbf{S}_{1,2}$ the matrices of space disrctetization, $\mathbf{E}, \mathbf{H}$ the vectors of electric and magnetic field probes in the inner area of region I, $\mathbf{E}_b$ the probes of electric field on the surface $\mathcal{S}$ given by (1) and (2), and $\boldsymbol{\varepsilon}_r$ and $\boldsymbol{\mu}_r$ the matrices of relative permittivity and permeability, respectively [24]. After simple algebraic manipulation of (4) and (5) we obtain the relation for $\mathbf{H}$ with respect to $\mathbf{E}_b$ which takes the form:

$$\mathbf{H} = -j\omega\varepsilon_0(\mathbf{G})^{-1}\mathbf{S}^{-1}\mathbf{P}_1\mathbf{D}_1\mathbf{Q}_b\mathbf{E}_b, \tag{6}$$

where $\mathbf{G} = \boldsymbol{\mu}_r^{-1}\mathbf{S}_1^{-1}\mathbf{P}_1\mathbf{D}_1\mathbf{Q}\boldsymbol{\varepsilon}_r^{-1}\mathbf{S_2}^{-1}\mathbf{P}_2\mathbf{D}_2 + \omega^2\mu_0\varepsilon_0\mathbf{I}$. Using the orthogonality of $e^{jm\varphi}$ function and taking each term of (1) as a boundary condition with arbitrary values of $c_{pm}^{E_z,\varphi}$, separately the unknown coefficients of magnetic field components expressed on surface $\mathcal{S}$ as:

$$H_{z,\varphi}^m(\rho = R, \varphi) = \sum_{l=-M}^{M} D_{lm}^{H_z,\varphi} e^{j(l\varphi - j\beta z)} \tag{7}$$

can be determined. Now, utilizing coefficients $C_m^{E_z,\varphi}$ and $D_{lm}^{H_z,\varphi}$ the impedance matrix $\mathbf{Z}$ can be obtained as follows:

$$\mathbf{Z} = (\mathbf{D}^{\mathbf{H}})^{-1}\mathbf{C}^{\mathbf{E}}, \tag{8}$$

where $\mathbf{C}^E$ is diagonal matrix and $\mathbf{D}^H$ is full matrix containing electric and magnetic field expansion coefficients, respectively.

To improve the accuracy of FDFD solution in the case of dielectric objects the effective dielectric constant algorithm [25] modified to cylindrical coordinates system [26] is applied. This algorithm assumes that in the mesh cells containing boundaries between regions with two different values of dielectric constants ($\varepsilon_1 \neq \varepsilon_2$) the effective dielectric constants are computed and these values are next used to update the ε_r matrix. In the analysis of ferrite materials the scheme presented in [27] is applied. In this scheme the mean and centered differentiation operator are combined together to utilize only the fields defined in Yee's grid.

3. DESIGN OF CFCL CIRCULATOR

The proposed structure of four-port circulator is presented in Fig. 4. It consists of a cascade connection of magic-T junction, cylindrical
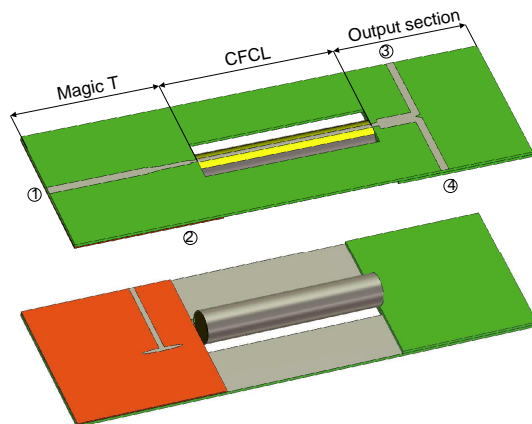
Figure 4. Top and bottom view of four-port circulator utilizing cylindrical ferrite coupled line junction.

coupled slotline junction (CFCL) and multilayer transformer from coupled slotlines to microstrip lines. In the design of the circulator the CFCL junction proposed in [10] and described in Section 3.1 was applied. Taking into account the dimensions of CFCL junction the feeding structures, i.e., magic-T junction and output transformer were designed and presented in Sections 3.2 and 3.3, respectively. The feeding structures were optimized with the use of commercial software HFSS. The overall scattering parameters of four-port CFCL circulator were predicted by cascading scattering matrices of the circulator components. The obtained results are presented and discussed in Section 3.4.

3.1. CFCL Section

In the design of four-port circulator the CFCL section presented in [10] was utilized. The angular dimensions of junction were slightly modified to obtain $\pi/4$ Faraday rotation angle for the length of ferrite section $L = 26$ mm at operation frequency $f_0 = 8.2$ GHz. The optimized values of angular slot and strip widths were $\Delta\varphi_s = 25°$ and $\Delta\varphi_p = 15°$, respectively.

In order to show the nonreciprocal behavior of the junction the power density and transversal field distribution in ferrite section were calculated using FDFD/MoM/MM approach and shown in Fig. 5. From the presented results it can be found that when the $\pi/4$ ferrite section is excited with the even mode (see Fig. 5(a)), the signal at
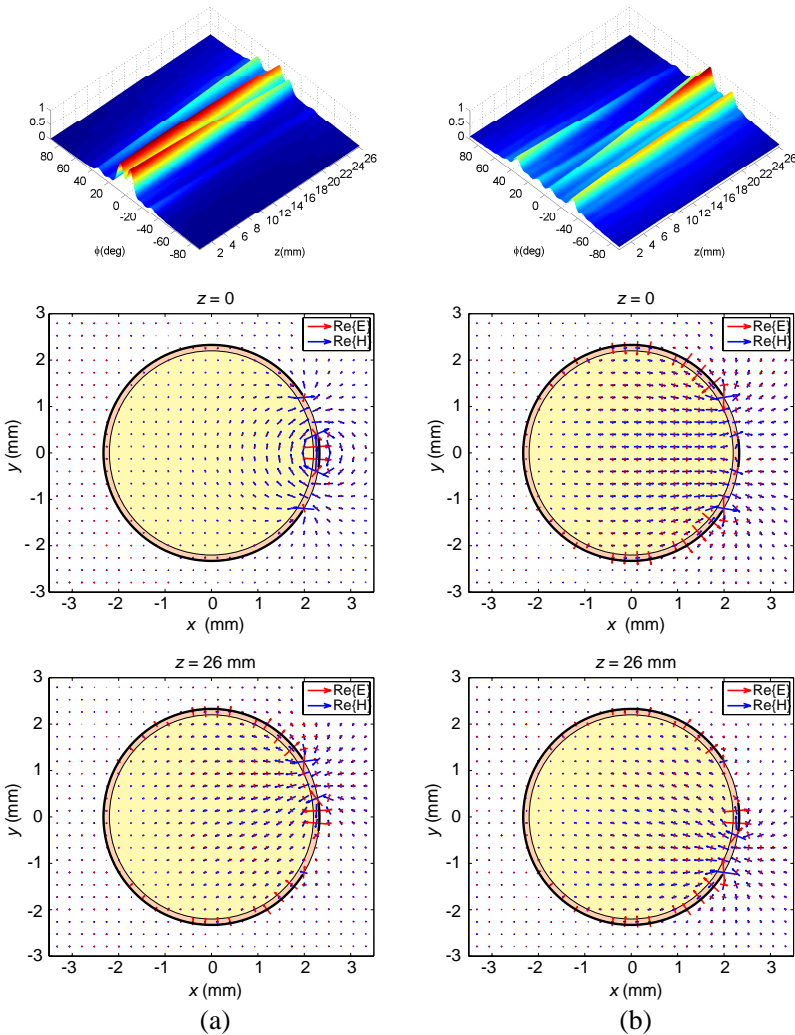
Figure 5. Power density and transversal field distribution in the ferrite coupled line section for (a) even and (b) odd mode excitation calculated at $f_0 = 8.2\,\mathrm{GHz}$.

the output ($z = 26\,\mathrm{mm}$) is concentrated in one slot of the cylindrical ferrite coupled slotlines. In the case of odd mode excitation of the ferrite section (see Fig. 5(b)), the power concentrates in the opposite slot of CFCL at the output.

For the investigated CFCL junction with ferrite section length $L =$
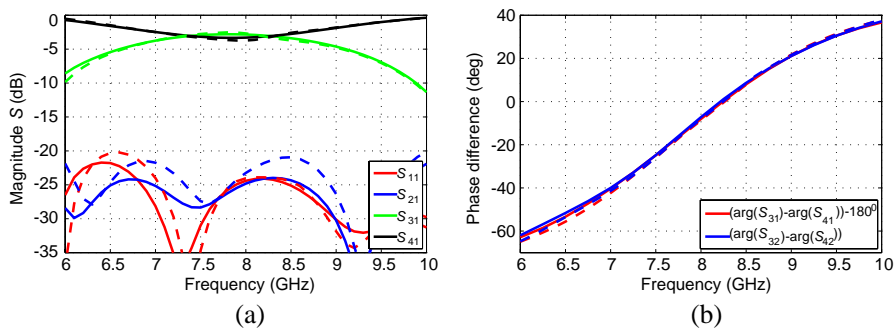
Figure 6. Scattering parameters of CFCL junction: (a) amplitude, (b) phase difference (solid line — our method, dashed line — HFSS).

26 mm the frequency dependent scattering parameters were calculated and presented in Fig. 6. From presented results it can be found that the designed section satisfy the amplitude and phase conditions [13] required for proper operation of FCL devices. The amplitude operation condition defined by 3 ± 0.5 dB power division is obtained in frequency range from 7 to 8.4 GHz. Moreover, when port (1) or (2) is excited, the phase difference between output signals appearing in ports (3) and (4) is close to optimal value $0/180°$ near the operation frequency 8.2 GHz. The results of analysis using FDFD/MoM/MM technique are compared with the ones obtained from commercial software HFSS and a good agreement is observed.

3.2. Magic-T Junction

In order to achieve even and odd excitation of CFCL junction the novel type of magic-T junction shown in Fig. 7 was proposed. This junction is a three-layer structure composed of slot layer (see Fig. 7(d)) placed between two substrates and two microstrip layers situated at the top and at the bottom of the structure (see Figs. 7(c) and 7(e)). When port (1) of the junction is excited the signals equal in amplitude and phase appear at ports (3) and (4) with port (2) of the structure being isolated (even mode excitation). On the other hand when port (2) of the junction is excited, the signal is coupled from microstrip line placed in a bottom layer (see Fig. 7(b)) to slotline located in a middle layer of the structure. In this case signals appearing in ports (3) and (4) are equal in amplitude and out of phase (odd mode excitation). In order to obtain high efficiency of the coupling from microstrip to slotline the patches with elliptical shapes were applied. Moreover in order to match the planar circuit to cylindrical junction $\pi/2$ impedance transformer was designed.
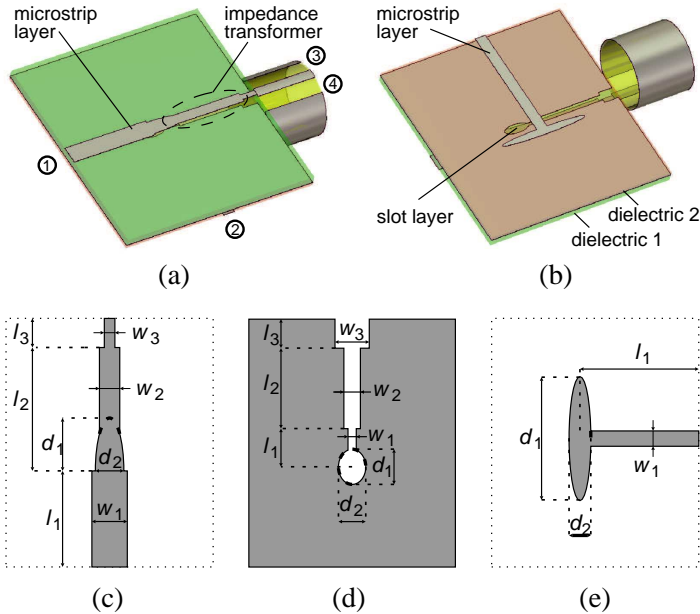
Figure 7. Multilayer magic T-junction: (a) top view, (b) bottom view, (c) top layer: $w_1 = 1.14$, $w_2 = 0.65$, $w_3 = 0.34$, $l_1 = 4.64$, $l_2 = 6.36$, $l_3 = 1$, $d_1 = 2.55$, $d_2 = 0.92$, (d) middle layer: $w_1 = 0.2$, $w_2 = 0.4$, $w_3 = 0.83$, $l_1 = 1.85$, $l_2 = 4.3$, $l_3 = 1$, $d_1 = 1.7$, $d_2 = 0.66$, and (e) bottom layer: $w_1 = 0.74$, $l_1 = 6$, $d_1 = 6.02$, $d_2 = 0.53$ (all dimensions are in millimeters). Parameters of dielectric substrates: $h_1 = 0.508\,\text{mm}$, $\varepsilon_{r1} = 3.5$, $h_2 = 0.254\,\text{mm}$, $\varepsilon_{r2} = 2.2$.

Utilizing the commercial software the dimensions of the structure were optimized for optimal performance of the junction. The simulated scattering parameters of the structure are presented in Fig. 8(a). From the presented results it can be found that for the considered junction the transmission is equal $-3\pm0.2\,\text{dB}$ with reflection losses and isolation better than $20\,\text{dB}$ in frequency range from 7.2 to 9.4 GHz.

3.3. Output Section

In the output of CFCL junction the transformer from coupled cylindrical slotlines to uncoupled planar microstrip lines was designed (see Fig. 9). The configuration of the structure is similar to the one presented in [10]. However, in comparison to [10] the substrate and overlay with low permittivity ($\varepsilon_r = 3.5$) were assumed, which allows for better matching of cylindrical section with planar one. Moreover,

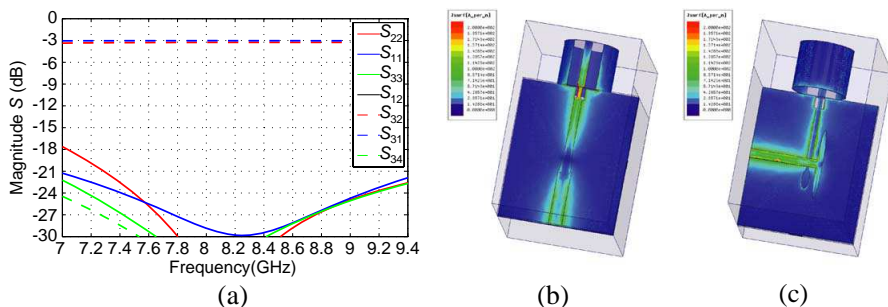(a)   (b)   (c)

Figure 8. Simulation results of magic T-junction: (a) frequency dependent scattering parameters characteristics and current distribution for the excitation in (b) port 1 and (c) port 2 of the investigated structure.
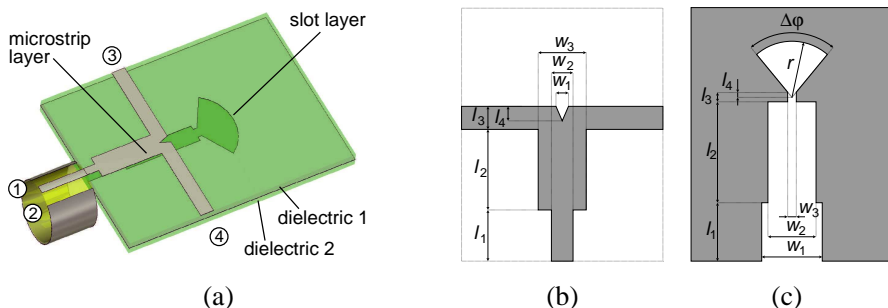

(a)   (b)   (c)

Figure 9. Multilayer coupled slotlines to microstrip lines transformer: (a) schematic view, (b) microstrip layer: $w_1 = 0.59$, $w_2 = 0.6$, $w_3 = 1.78$, $l_1 = 1$, $l_2 = 5.24$, $l_3 = 1.14$, $l_4 = 0.83$, and (c) slot layer: $w_1 = 1.02$, $w_2 = 1.42$, $w_3 = 0.75$, $l_1 = 3.3$, $l_2 = 6.51$, $l_3 = 0.33$, $l_4 = 0.23$, $r = 3.23$, $\Delta\varphi = 116°$ (all dimensions are in millimeters). Parameters of dielectric substrates: $\varepsilon_{r1} = \varepsilon_{r2} = 3.5$, $h_1 = h_2 = 0.508$ mm.

using substrates with low permittivity the reduction of phase shift between even and odd mode propagating in planar coupled lines of the structure can be obtained. As a result this allows to increase the isolation between ports (1)–(4) and (3)–(2) required for proper operation of the circulator.

    The layout of the structure was optimized with the use of commercial software HFSS. The results of simulation are presented in Fig. 10. It can be found that for optimized transformer the isolation and reflection losses are better than 20 dB in the considered frequency range from 7.4 to 9 GHz.
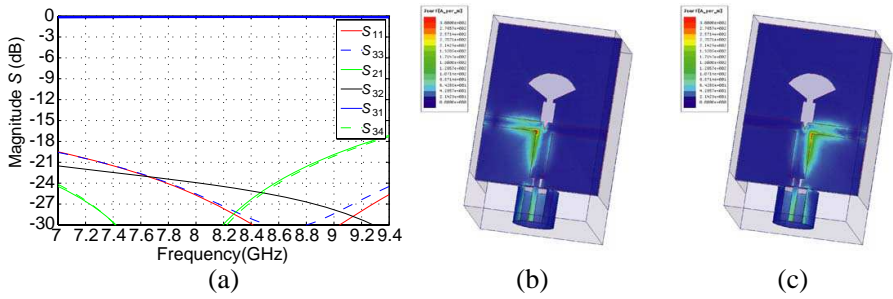
Figure 10. Simulation results of multilayer coupled slotlines to microstrip lines transformer: (a) frequency dependent scattering parameters characteristics and current distribution for the excitation in (b) port 1 and (c) port 2 of the investigated structure.
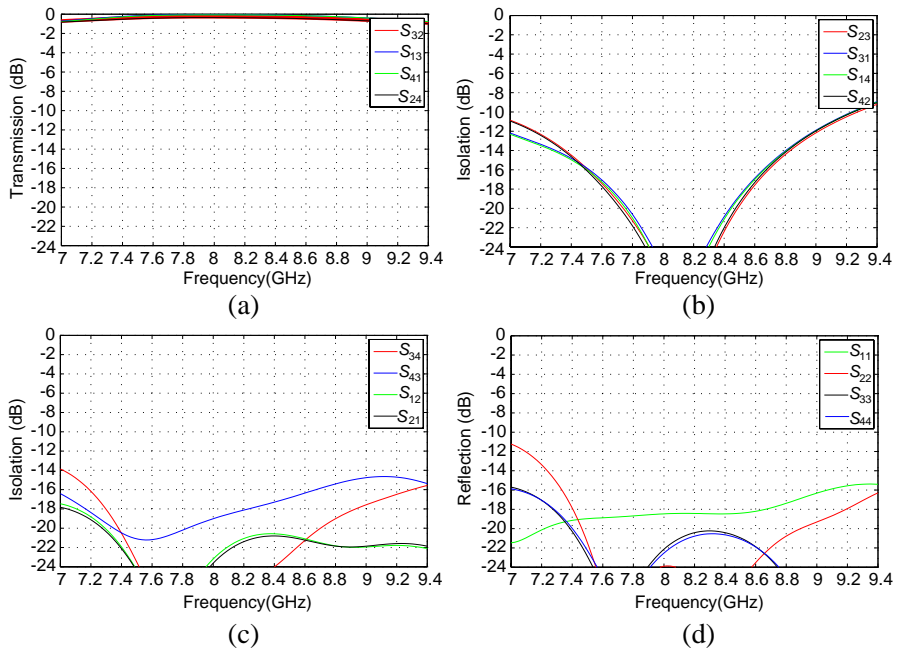

Figure 11. Simulated scattering parameters of four-port CFCL circulator: (a) transmission, (b) isolation, (c) coupling between neighboring ports and (d) reflection coefficients.
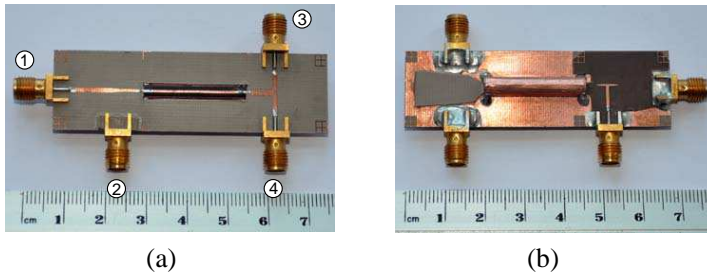
Figure 12. Photograph of fabricated four-port CFCL circulator: (a) top view, (b) bottom view.

3.4. Four-port Circulator

The frequency dependent scattering parameters of the circulator were calculated by cascading scattering matrices of its components and are shown in Fig. 11. From the presented results it can be found that the isolation and reflection losses are better than 18 dB in frequency range from 7.6 to 8.6 GHz. In the simulation of CFCL circulator parameters, the lossless ferrite junction was considered. The losses in FCL devices arise mainly from ferrite section. For the investigated configuration of CFCL junction the ferrite and conductor losses were estimated with the use of commercial software in [10] and were about 0.23 dB.

4. EXPERIMENTAL RESULTS

The designed circulator was fabricated. The planar layers of the circulator were positioned each other manually with the use of additional markers. The structure of CFCL junction was fabricated by etching the circuit on thin dielectric planar substrate and then folding it on a dielectric/ferrite circular cylinder. Photograph of circulator prototype is presented in Fig. 12. During the measurements the ferrite cylinder was magnetized with the use of magnet system. The measured scattering parameters of four-port CFCL circulator are shown in Fig. 13. From the presented results it is seen that the transmission from port (1) to (4) and (3) to (1) is better than -1.5 dB and the transmission from port (2) to (3) and from port (4) to (2) is better than -3 dB in frequency range 7.6 to 8.6 GHz. In this frequency range the isolation between aforementioned pairs of ports is better than 12 dB with reflection losses better than 8 dB. The isolation between ports (1)–(2) and (3)–(4) is better then 10 dB. The higher level of reflection and insertion losses which are observed in
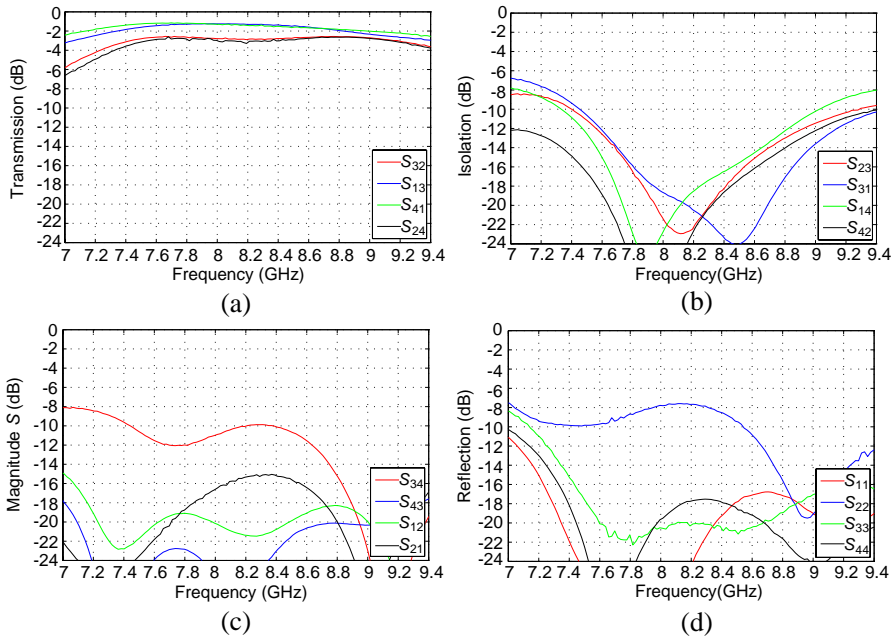
Figure 13. Measured scattering parameters of four-port CFCL circulator: (a) transmission, (b) isolation, (c) coupling between neighboring ports, and (d) reflection coefficients.

measured scattering parameters associated with port 2 are caused by the inaccuracies of manufacturing and assembling process. The most significant influence on deteriorating performance of the circulator has the proper positioning of cylindrical section with respect to planar circuits. Nevertheless the obtained results of measurements well agree with the results of simulation.

It should be noted that the measured fractional bandwidth of circulator is similar to the bandwidth achieved for the planar four-port circulator utilizing hybrid coupler [11] and is equal 20%. The advantage of proposed circulator over the aforementioned planar one are considerably lower insertion losses $(1.5 \div 3\,\text{dB})$ and dimensions of the structure (printed circuit board: $20 \times 65\,\text{mm}$ $(0.55 \times 1.78\lambda_0)$). For the structure from [11] the measured insertion losses at operation frequency $f_0 = 11\,\text{GHz}$ were $8\,\text{dB}$ and the dimensions of printed circuit board were $29 \times 75\,\text{mm}$ $(1.06 \times 2.75\lambda_0)$.

5. CONCLUSION

In this paper the numerical and experimental investigations of four-port circulator utilizing single cylindrical ferrite coupled CFCL line junction were presented for the first time. The investigated structure of circulator was obtained by cascading magic-T junction with cylindrical ferrite junction and output transformer from cylindrical coupled slotlines to uncoupled planar microstrip lines. Due to the cylindrical geometry of junction the new type of multilayer magic-T junction and output transformer were developed. Moreover, in order to efficiently and accurately analyze CFCL junction the hybrid FDFD/MoM/MM technique was proposed. The designed structure of circulator was fabricated and measured. A good agreement between simulated results and measured ones was obtained.

ACKNOWLEDGMENT

REFERENCES

1. Yang, L.-Y. and K. Xie, "Design and measurement of nonuniform ferrite coupled line circulator," *Journal of Electromagnetic Waves and Applications*, Vol. 25, No. 1, 131–145, 2011.

2. Queck, C. K. and L. E. Davis, "Broad-band three-port and four-port stripline ferrite coupled line circulators," *IEEE Transactions on Microwave Theory and Techniques*, Vol. 52, No. 2, 625–632, Feb. 2004.

3. Marynowski, W. and J. Mazur, "Study of nonreciprocal devices using three-strip ferrite coupled line," *Progress In Electromagnetics Research*, Vol. 118, 487–504, 2011.

4. Cao, M. and R. Pietig, "Ferrite coupled-line circulator with reduced length," *IEEE Transactions on Microwave Theory and Techniques*, Vol. 53, No. 8, 2572–2579, Aug. 2005.

5. Kusiek, A., W. Marynowski, and J. Mazur, "Investigations of the circulation effects in the structure using ferrite coupled slot-line section," *Microwave and Optical Technology Letters*, Vol. 49, No. 3, 692–696, Jan. 2007.

6. Mazur, J., M. Solecka, R. Poltorak, and M. Mazur, "Theoretical and experimental treatment of a microstrip coupled ferrite line circulator," *IEE Proceedings — Microwaves, Antennas and Propagation*, Vol. 151, No. 6, 477–480, Dec. 2004.

7. Mazur, J., M. Mazur, J. Michalski, and E. Sedek, "Isolator using a ferrite-coupled-lines gyrator," *IEE Proceedings — Microwaves, Antennas and Propagation*, Vol. 149, Nos. 5–6, 291–294, Oct./Dec. 2002.

8. Marynowski, W., A. Kusiek, and J. Mazur, "Microstrip ferrite coupled line isolators," *XVI International Microwaves, Radar and Wireless Communications Conference*, Vol. 1, 342–345, Krakow, Poland, May 2006.

9. Marynowski, W., A. Kusiek, and J. Mazur, "Microstrip four-port circulator using a ferrite coupled line section," *AEU — International Journal of Electronics and Communications*, Vol. 63, No. 9, 801–808, Jul. 2008.

10. Kusiek, A., W. Marynowski, and J. Mazur, "Investigations of nonreciprocal devices employing cylindrical ferrite coupled line junction," *Journal of Electromagnetic Waves and Applications*, Vol. 26, No. 13, 1685–1693, 2012.

11. Queck, C. K. and L. E. Davis, "Microstrip and stripline ferrite-coupled-lines (FCL) circulators," *IEEE Transactions on Microwave Theory and Techniques*, Vol. 50, No. 12, 2910–2917, Dec. 2002.

12. Mazur, J. and M. Mrozowski, "On the mode coupling in longitudinally magnetized waveguiding structures," *IEEE Transactions on Microwave Theory and Techniques*, Vol. 37, No. 1, 159–164, Jan. 1989.

13. Mazur, J., M. Mazur, and J. Michalski, "Coupled-mode design of ferrite-loaded coupled-microstrip-lines section," *IEEE Transactions on Microwave Theory and Techniques*, Vol. 50, No. 6, 1487–1494, Jun. 2002.

14. Chiang, C. T. and B.-K. Chung, "Ultra wideband power divider using tapered line," *Progress In Electromagnetics Research*, Vol. 106, 61–73, 2010.

15. Zhang, H., X.-W. Shi, F. Wei, and L. Xu, "Compact wideband gysel power divider with arbitrary power division based on patch type structure," *Progress In Electromagnetics Research*, Vol. 119, 395–406, 2011.

16. Sedighy, S. H. and M. Khalaj-Amirhosseini, "Compact Wilkinson power divider using stepped impedance transmission lines," *Journal of Electromagnetic Waves and Applications*, Vol. 25,

No. 13, 1773–1782, 2011.

17. Liu, G.-Q., L.-S. Wu, and W.-Y. Yin, "A compact microstrip rat-race coupler with modified lange and T-shaped arms," *Progress In Electromagnetics Research*, Vol. 115, 509–523, 2011.

18. Li, Q., X.-W. Shi, F. Wei, and J. G. Gong, "A novel planar 180° out-of-phase power divider for UWB application," *Journal of Electromagnetic Waves and Applications*, Vol. 25, No. 1, 161–167, 2011.

19. Kazerooni, M. and M. Aghalari, "Size reduction and harmonic suppression of rat-race hybrid coupler using defected microstrip structure," *Progress In Electromagnetics Research Letters*, Vol. 26, 87–96, 2011.

20. Deng, P.-H., J.-H. Guo, and W.-C. Kuo, "New Wilkinson power dividers based on compact stepped-impedance transmission lines and shunt open stubs," *Progress In Electromagnetics Research*, Vol. 123, 407–426, 2012.

21. Davidovitz, M., "A compact planar magic-T junction with aperture-coupled difference port," *IEEE Microwave and Guided Wave Letters*, Vol. 7, No. 8, 217–218, Aug. 1997.

22. Marynowski, W. and J. Mazur, "Investigation of multilayer magic-T configurations using novel microstrip-slotline transitions," *Progress In Electromagnetics Research*, Vol. 129, 98–108, 2012.

23. Kusiek, A., W. Marynowski, and J. Mazur, "Investigations of cylindrical ferrite coupled line junction using hybrid technique," *Progress In Electromagnetics Research*, Vol. 120, 143–164, 2011.

24. Kusiek, A. and J. Mazur, "Analysis of scattering from arbitrary configuration of cylindrical objects using hybrid finite-difference mode-matching method," *Progress In Electromagnetics Research*, Vol. 97, 105–127, 2009.

25. Kaneda, N., B. Housmand, and T. Itoh, "FDTD analysis of dielectric resonators with curved surfaces," *IEEE Transactions on Microwave Theory and Techniques*, Vol. 45, No. 9, 1645–1649, Sep. 1997.

26. Kowalczyk, P., M. Wiktor, and M. Mrozowski, "Efficient finite difference analysis of microstructured optical fibers," *Optics Express*, Vol. 13, No. 25, 10349–10359, Dec. 2005.

27. Garcia, S. G., T. M. Hung-Bao, R. G. Martin, and B. G. Olmedo, "On the application of finite methods in time domain to anisotropic dielectric waveguides," *IEEE Transactions on Microwave Theory and Techniques*, Vol. 44, No. 12, 2195–2206, Dec. 1996.